AAC Journals.ASM.org

Substitutions at Position 105 in SHV Family β-Lactamases Decrease Catalytic Efficiency and Cause Inhibitor Resistance

Mei Li,[a] Benjamin C. Conklin,[a] Magdalena A. Taracila,[a] Rebecca A. Hutton,[a] and Marion J. Skalweit[a,b,c]

Louis Stokes Cleveland Department of Veterans Affairs Medical Center[a] and Departments of Medicine[b] and Biochemistry,[c] Case Western Reserve University School of Medicine, Cleveland, Ohio, USA

Ambler position 105 in class A β-lactamases is implicated in resistance to clavulanic acid, although no clinical isolates with mutations at this site have been reported. We hypothesized that Y105 is important in resistance to clavulanic acid because changes in positioning of the inhibitor for ring oxygen protonation could occur. In addition, resistance to bicyclic 6-methylidene penems, which are interesting structural probes that inhibit all classes of serine β-lactamases with nanomolar affinity, might emerge with substitutions at position 105, especially with nonaromatic substitutions. All 19 variants of SHV-1 with variations at position 105 were prepared. Antimicrobial susceptibility testing showed that *Escherichia coli* DH10B expressing Y105 variants retained activity against ampicillin, except for the Y105L variant, which was susceptible to all β-lactams, similar to the case for the host control strain. Several variants had elevated MICs to ampicillin-clavulanate. However, all the variants remained susceptible to piperacillin in combination with a penem inhibitor (MIC, ≤2/4 mg/liter). The Y105E, -F, -M, and -R variants demonstrated reduced catalytic efficiency toward ampicillin compared to the wild-type (WT) enzyme, which was caused by increased K_m. Clavulanic acid and penem K_i values were also increased for some of the variants, especially Y105E. Mutagenesis at position 105 in SHV yields mutants resistant to clavulanate with reduced catalytic efficiency for ampicillin and nitrocefin, similar to the case for the class A carbapenemase KPC-2. Our modeling analyses suggest that resistance is due to oxyanion hole distortion. Susceptibility to a penem inhibitor is retained although affinity is decreased, especially for the Y105E variant. Residue 105 is important to consider when designing new inhibitors.

Resistance mediated by β-lactamase enzymes continues to be an important problem in hospitals. In general, β-lactamase enzymes are categorized by either amino acid sequence (Ambler method) as classes A to D or by function (Bush-Jacoby-Medeiros) as groups 1a to 3b (4). Among the well-studied class A β-lactamases, 143 SHV and 185 TEM clinically derived β-lactamases have been described to date (reviewed and cataloged by G. Jacoby and K. Bush, http://www.lahey.org/Studies/). The major phenotypic divisions among the SHV and TEM enzymes are the extended-spectrum β-lactamases (ESBLs) (functional class 2be) and the inhibitor-resistant β-lactamases (functional class 2br). As a general rule, ESBLs exhibit greater susceptibility to inhibition by class A β-lactamase inhibitors, especially clavulanic acid. Another class A example, the CTX-M β-lactamases, are potent cefotaximases and are readily inhibited by tazobactam. Thus far, "inhibitor resistance" has been described mainly in the TEM β-lactamases, with certain single amino acid substitutions particularly associated with the resistance phenotype (M69I, -L, and -V, S130G, and R244S). The S130G mutants and the M69I mutant have also been reported in SHV (13, 27, 40; GenBank accession number AY265888 [partial sequence]): SHV-10 (G54 del, S130G, A140R, K192N, L193V, G238S, and E240K), SHV-49 (M69I), SHV-52 (T18A, L35Q, M69I, and T141I), and SHV-92 (L35Q, M69I, T141I), as well as new inhibitor-resistant enzymes with the K234R substitution (14, 28, 30, 31). These enzymes are rarely encountered in the clinic, although resistance to clavulanic acid in both the TEM and SHV mutants is easy to demonstrate. The enzymes generally retain activity versus ampicillin. A small number of so-called "complex mutants" (functional class 2ber) that contain both phenotypes have been described as well. Generally such enzymes show increased resistance to clavulanic acid and an increased ability to hydrolyze ceftazidime. Finally, there are also newer class A carbapenemases (functional group 2f) such as the KPC group of enzymes, which have broad-spectrum hydrolytic activity and are resistant to clinically available β-lactamase inhibitors, including tazobactam (3, 35–37, 45, 46), and GES-1 and GES-5, which show resistance to clavulanic acid (16).

The role of residue 105 in class A β-lactamases was reviewed by Page (34). Page speculated based on examination of a series of class A enzymes that aromatic residues at position 105 created a hydrophobic "wall" to allow protonation of clavulanic acid during its inhibition chemistry. Enzymes that naturally lacked a hydrophobic residue at this position were resistant to clavulanic acid inhibition (34). The position of tyrosine 105 in SHV can also be affected by substitutions at position 104, which alter its interaction with the thiazolidine ring of penicillin substrates (1). More recently, an analysis of TEM Y105D, -G, -N, and -W substituted β-lactamases suggested that less rigid side chain residues such as aspartate led to poor positioning of substrates in the active site (8–10). Inhibitors were not studied with TEM variants having variations at residue 105. The KPC-2 enzyme was also studied in great detail with site saturation mutagenesis at position 105, which revealed preserved hydrolytic activity but resistance to clavulanic acid with increased partition ratios for the variants that had increased clavulanic acid MICs (37). However, all of the strains ex-

Received 3 April 2012 Returned for modification 17 June 2012
Accepted 13 August 2012
Published ahead of print 20 August 2012
Address correspondence to Marion J. Skalweit, marion.skalweit@case.edu.

doi:10.1128/AAC.00711-12

TABLE 1 Primers used in this study

Primer	Sequence[a]
SHV-1 Y105X	
Forward	5′-GCAGGATCTGGTGGAC**NNS**TCGCCGGT CAGCGAAA-3′
Reverse	5′-TTTCGCTGACCGGCGA**SNN**GTCCACCA GATCCTGC-3′
Y105C	
Forward	5′-GCAGGATCTGGTGGAC**TGC**TCGCCGGT CAGCGAAA-3′
Reverse	5′-TTTCGCTGACCGGCGA**CGA**GTCCACCA GATCCTGC-3′
Y105F	
Forward	5′-GCAGGATCTGGTGGAC**TTC**TCGCCGGT CAGCGAAA-3′
Reverse	5′-TTTCGCTGACCGGCGA**GAA**GTCCACCA GATCCTGC-3′
Y105I	
Forward	5′-GCAGGATCTGGTGGAC**ATC**TCGCCGGT CAGCGAAA-3′
Reverse	5′-TTTCGCTGACCGGCGA**GAT**GTCCACCAG ATCCTGC-3′
Y105T	
Forward	5′-GCAGGATCTGGTGGAC**ACC**TCGCCGGTC AGCGAAA-3′
Reverse	5′-TTTCGCTGACCGGCGA**GGT**GTCCACCAGA TCCTGC-3′

[a] Boldface indicates site of codon substitution.

pressing 105-substituted KPC-2 enzymes showed increased susceptibility to piperacillin-tazobactam compared to the strain containing wild-type (WT) KPC-2. These studies suggest that Y105 interactions with substrates and inhibitors are equally important and may explain the absence of clinical inhibitor-resistant mutants with mutations at the 105 site. This has important implications in the design of β-lactamase inhibitors, since inhibitors that rely on residue 105 for positioning are potentially protected against resistance mutations since such mutations will be deleterious to the overall catalytic efficiency of the enzyme. If this behavior is common to diverse class A enzymes such as KPC and SHV, then it can be used to great advantage in the design of additional broad-spectrum inhibitors of class A β-lactamases.

With this in mind, we set out to further understand the interactions of residue Y105 in SHV β-lactamase with substrates and inhibitors of class A β-lactamases.

MATERIALS AND METHODS

Mutagenesis and MIC determinations for *Escherichia coli* expressing SHV Y105Xaa. Variants with changes at position 105 in SHV-1 β-lactamase were prepared by site saturation mutagenesis using a Stratagene QuikChange kit with bla_{SHV-1} directionally subcloned in pBCSK(−) vector as previously described (18) and were confirmed by DNA sequencing of 96 randomly selected clones. Mutagenesis primers (Table 1) were designed based on the SHV-1 sequence (*Klebsiella pneumoniae* β-lactamase SHV-1 gene, accession number AF124984) and common codon usage in *K. pneumoniae* (21). Both strands of the entire bla_{SHV-1} gene were sequenced using the commercially available M13Forward and M13Reverse primers for pBSK(−) for each variant. The Y105C, -F, -I, and -T variants were prepared using site-directed mutagenesis.

MIC determinations (see Tables 2 and 3) were conducted for all 19 position 105 variants by agar dilution using ampicillin (Sigma), piperacillin (Sigma), ceftazidime (Hoffman-LaRoche), ceftriaxone (Sigma), cephalothin (Sigma), ampicillin with clavulanic acid (Sigma), sulbactam (a kind gift of Pfizer) and tazobactam, keeping the ampicillin concentration fixed at 50 mg/liter (a kind gift of Pfizer), piperacillin with tazobactam, and penem-1 (a kind gift of Pfizer) (5, 37, 39).

Immunoblots. *E. coli* DH10B cells transformed with pBC SK(−) *bla*SHV-1 with all 19 Y105 variants and the WT were grown in lysogeny broth (LB) to an optical density at 600 nm (OD_{600}) of 0.8. A 5-ml portion with this cell density was pelleted at 12,000 rpm for 2 min. After the supernatant was discarded, the pellet was resuspended in 80 μl of 5× sodium dodecyl sulfate-polyacrylamide gel electrophoresis (SDS-PAGE) loading dye. Sample volumes of 10 μl were loaded into each lane of an SDS-polyacrylamide gel. The gel was run and transferred to a polyvinylidene difluoride membrane. The membrane was blocked overnight at 4°C in 200 ml of blocking buffer (15 g nonfat dry milk dissolved in 300 ml Tris-buffered saline [TBS] [20 mM Tris-Cl, pH 7.4, with 150 mM NaCl]). The membrane was then incubated for 2 h at room temperature while shaking with polyclonal anti-SHV-1 rabbit antibody (18, 22, 23) at 1.0 μg/ml in blocking buffer. The membrane was washed with TBS containing 0.05% Tween 20 (TBS-T) four times for 10 min each and then incubated with protein G-horseradish peroxidase conjugate (Bio-Rad) for 1 h at room temperature with shaking. The blot was washed again with TBS-T four times for 10 min each and then developed using the ECL developing kit (GE Healthcare Life Sciences) according to the manufacturer's instructions. The gels were analyzed using Image J software (http://rsb.info.nih.gov/ij), and expression levels were normalized to the level of WT expression.

Expression and purification of SHV Y105X variants. The Y105R, -E, -M, and -F variants were expressed in *E. coli* DH10B (Invitrogen) by growing up 1.6 liters of overnight cultures in LB with 20 mg/liter added chloramphenicol. β-Lactamases were extracted as previously described (18) by spinning down and freezing cell pellets and using lysozyme and EDTA for limited periplasmic fractionation (18). Crude extracts were used directly in preparative isoelectric focusing gels with pH 3.5 to 10 ampholines (Bio-Rad). β-Lactamase protein bands were identified with nitrocefin (NCF) (Becton Dickinson, Cockeysville, MD) and excised. β-Lactamase protein was eluted with 1× phosphate-buffered saline (PBS), pH 7.4. Proteins were further purified by gel filtration or anion-exchange chromatography using Sephadex with 1× PBS (pH 7.4) or GE HiTrap Q HP columns with 50 mM Tris HCl and 50 mM Tris HCl plus 1 M NaCl, both pH 9.6. The gradient was 15% Tris plus NaCl over 25 5-ml column volumes. Protein purity was assessed with SDS-polyacrylamide gels and was >95%. Samples were concentrated and then used directly in kinetic assays. Protein concentrations were determined by Bradford assay using bovine serum albumin as a standard (2). The purification strategy employed yielded several milligrams of natively folded proteins (WT and Y105E, -M, -R, and -F) with greater than 95% purity as assessed by SDS-PAGE.

β-Lactamase hydrolysis assays and inhibition assays. Standard multiple-turnover kinetic analyses of reaction velocity versus substrate concentration were performed using 7 to 10 nM SHV protein in 10 mM PBS. β-Lactam hydrolysis was monitored at room temperature using an Agilent 8453 diode array spectrophotometer in a total reaction volume of 1 ml. Measurements were obtained using NCF (Becton Dickinson, Cockeysville, MD) ($\Delta\varepsilon_{482}$ = 17,400 M^{-1} cm^{-1}), ampicillin (Sigma) ($\Delta\varepsilon_{235}$ = −900 M^{-1} cm^{-1}), cephalothin (Sigma) ($\Delta\varepsilon_{262}$ = −7,660 M^{-1} cm^{-1}), and cefoperazone (Sigma) ($\Delta\varepsilon_{275}$ = −8,640 M^{-1} cm^{-1}). Steady-state kinetic parameters V_{max} and K_m were obtained by fitting reaction curves to the Henri-Michaelis-Menten equation using Origin 8.0. When hydrolysis could not be measured directly, a competition assay using NCF as a reporter substrate was performed and a K_d (dissociation constant) reported for the compound, correcting for NCF affinity (11). We initiated the reaction with addition of enzyme to a mixture of NCF and the poor

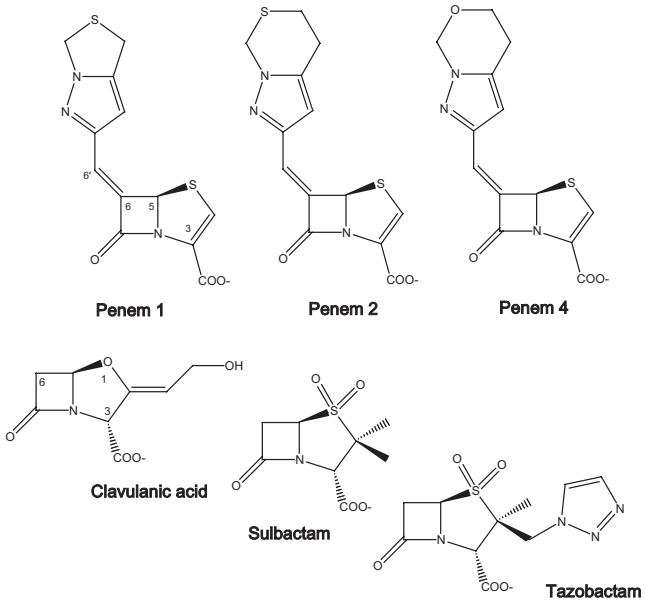

FIG 1 Inhibitors used in this study.

substrate and took initial velocity measurements during the first 5 to 10 s of the progress curves to better approximate formation of the Henri-Michaelis-Menten complex (43).

The inhibitors used in our assays are shown in Fig. 1. They are mechanism-based "suicide inhibitors" that form several different long-lived covalent adducts with the enzymes. The K_i value was determined using the Dixon method (7). For both the K_i and K_d determinations, we initiated the reaction with addition of enzyme to a mixture of nitrocefin and inhibitor, assumed that rapid equilibration was occurring, and took initial velocity measurements for the first 5 to 10 s of the reaction to approximate formation of the enzyme-inhibitor complex, varying the concentrations of both the inhibitor and substrate.

We determined K_i values for each of the variants of interest and determined a rate of inhibition of the enzyme (k_{inh}) over a 5-min time course at K_i concentration of inhibitor for each variant enzyme, using [NCF] $\sim 5 \times K_m$ of the particular variant. This rate of inhibition, k_{inh}, over the initial 5 min of inhibition reflects the rate of formation of species important during this early time point.

Raman spectroscopy. Crystals of WT SHV were prepared by the hanging-drop method using 5 mg/ml SHV-1 in 1 mM HEPES buffer (pH 7.0), polyethylene glycol 8000 (PEG8000) in 100 mM HEPES (pH 7.0) (18%, wt/vol), and CYMAL-6 as previously described (19). Raman difference spectra of penem-1 inhibitor, SHV–penem-1 acyl enzyme complexes, and a hydrolysate of penem-1 prepared with 1 N NaOH were obtained using a Kaiser optical Raman microscope with a Coherent Innova C Kr ion laser at 647 nm as the excitation source. Difference spectra were generated using GRAMS AI spectral subtraction software as in prior studies (19).

Molecular modeling. To create models of protein-inhibitor complexes, the Protein Data Bank (PDB) structure of SHV-1 (1SHV) was minimized using DS 2.1 (Accelrys, Inc. San Diego, CA) molecular modeling software as previously described (35). The "proteins reports and utility" tools were used to correct crystallographic disorder, remove all alternate conformations, add missing atoms, and correct connectivity and bond order. The crystallographic waters were removed, and the enzyme was immersed in a box of water at 7 Å from any face of the box (Solvation module of DS 2.1) using Explicit Periodic Boundary conditions. The complex was minimized in several steps using Steepest-Descendant and Conjugate Gradient algorithms to reach the minimum convergence [0.01 kcal/(mol · Å)]. All energy minimizations and molecular dynamics simulations of the enzyme and enzyme complexes were carried out using the force-field parameters of CHARMm. The Particle Mesh Ewald method was used to treat long-range electrostatic interactions, and bonds that involved hydrogen atoms were constrained with SHAKE algorithm. The 1ONG (SHV-1 with 1,4-thiazepine intermediate–penem-4, O instead of S in the bicyclic ring) structure was used to prepare the molecular modeling of the SHV-1 penem-2 acyl enzyme complex. Penem-2 was studied because it could easily be modeled using an existing crystal structure coordinate set (1ONG) and because it yields the same Raman intermediate as seen with penem-1. The X-ray structure was prepared in a manner similar to that for 1SHV as described above.

Docking and formation of the acyl enzyme complex. A model of the acyl enzyme complex of the SHV-1 enzyme and penem-2 was constructed. The 7-member thiazepine ring intermediate of the penem-2 structure was built using Fragment Builder tools. The CHARMm force field was applied; the molecule was solvated and minimized using the Standard Dynamics Cascade protocol. The thiazepine intermediate was docked in the active site of SHV-1 using the LibDock1 protocol of DS 2.1. Here, the multiple conformations of the ligand are docked into the active site of the enzyme, the complexes optimized, and the final poses scored. The 95 possible conformations (poses) were analyzed based on score, and one with the minimum distance between C7 (carbonyl group) and the catalytic S70 (oxygen) at 3.4 Å was chosen. The acyl complex was created, solvated, and minimized. The mutations at position 105 were created using the Build module of DS 2.1.

RESULTS

Mutagenesis, DNA sequencing, and susceptibility testing. DNA sequencing yielded 15 variants. No other mutations were observed in the SHV genes. The remaining variants (Y105C, -F, -I, and -T) were prepared by site-directed mutagenesis. The most frequently used codons in SHV-1 were selected. Mutagenized DNA in the phagemid vector pBC SK(−) was transformed into *E. coli* DH10B, and susceptibility testing was performed to assess the effect of the mutation on MICs. Controls included *E. coli* DH10B with wild-type SHV-1 β-lactamase and *E. coli* DH10B. The results of MIC testing are shown in Tables 2 and 3, with modal MIC values for 3 to 6 determinations.

MIC testing showed that many of the *E. coli* DH10B mutants

TABLE 2 MICs for Y105 SHV variants

Strain	Modal MIC (mg/liter)[a]						
	AMP	AMP50/CLAV	AMP50/SUL	AMP50/TAZO	CRO	CAZ	CF
DH10B	4	No growth	No growth	No growth	0.25	0.5	1
SHV-1	>16,384	2	256	>32	0.5	32	64
Y105A	128	1	2	8	0.5	0.5	2
Y105C	128	1	4	16	0.5	0.5	16
Y105D	1,024	8	32	>32	0.5	0.5	8
Y105E	1,024	16	64	>32	0.5	0.5	8
Y105F	16,384	4	64	>32	1	2	32
Y105G	512	2	4	32	0.5	0.5	16
Y105H	256	1	4	4	0.5	0.5	4
Y105I	1,024	2	4	32	0.5	0.5	16
Y105K	512	2	2	16	0.25	0.5	8
Y105L	32	No growth	No growth	No growth	0.5	0.5	8
Y105M	2,048	8	32	32	0.5	0.5	32
Y105N	512	2	16	16	0.5	0.5	32
Y105P	4,096	8	16	32	0.5	0.5	32
Y105Q	256	1	4	8	0.5	0.5	32
Y105R	1,024	4	16	16	2	0.5	32
Y105S	2,048	8	32	>32	0.5	0.5	16
Y105T	1,024	2	16	>32	0.5	0.5	16
Y105V	512	1	16	32	0.5	0.5	32
Y105W	8,192	1	64	>32	0.5	2	32

[a] Values are averages of 3 to 6 determinations. AMP, ampicillin; AMP50, ampicillin fixed at 50 mg/liter; AMP50/CLAV, ampicillin fixed at 50 mg/liter with various clavulanic acid amounts; AMP50/SUL, ampicillin fixed at 50 mg/liter with various sulbactam amounts; AMP50/TAZO, ampicillin fixed at 50 mg/liter with various tazobactam amounts; CRO, ceftriaxone; CAZ, ceftazidime; CF, cephalothin.

TABLE 3 MICs of piperacillin and piperacillin-inhibitor combinations for Y105 variants

Strain	MIC (mg/liter)[a]		
	PIP	PIP/TAZO	PIP/penem
DH10B	2	2	2
SHV-1	2,048	>512	2
Y105A	128	16	2
Y105C	32	16	2
Y105D	16	8	2
Y105E	32	4	2
Y105F	512	512	2
Y105G	128	32	2
Y105H	128	8	2
Y105I	256	8	2
Y105K	16	8	2
Y105L	32	8	2
Y105 M	512	16	2
Y105N	256	32	2
Y105P	256	32	2
Y105Q	128	16	2
Y105R	128	32	2
Y105S	256	64	2
Y105T	128	32	<2
Y105V	256	64	<2
Y105W	1,024	>512	<2

[a] Values are modes of 3 determinations. PIP, piperacillin; PIP/TAZO, piperacillin-tazobactam with a fixed tazobactam concentration of 4 mg/liter; PIP/penem, piperacillin–penem-1 with fixed penem-1 concentration of 4 mg/liter.

expressing Y105 variants were resistant to ampicillin (≥32 mg/liter), except for that expressing the Y105L variant. The Y105F and -W variant-expressing strains had the highest MICs toward ampicillin (16,384 and 8,192 mg/liter, respectively). Several variant-expressing strains had higher MICs (>50/2 mg/liter) then WT-expressing strains to ampicillin-clavulanate. These variants included Y105D, -E, -F, -M, -P, -R, and -S. These variants also showed increased MICs for combinations of ampicillin at 50 mg/liter with sulbactam or tazobactam at various concentrations, although the WT SHV-1-expressing strain also showed elevated MICs with these inhibitors compared to those with clavulanic acid. Pairing the inhibitors with the same β-lactam (e.g., ampicillin) allows one to observe subtle differences in the MIC effect of the inhibitors (36). The Y105A-, -F-, -G-, -H-, -I-, -M-, -N-, -P-, -Q-, -R-, -S-, -T-, -V-, and -W-containing strains were resistant to piperacillin (≥128 mg/liter), with the Y105F- and -W-expressing strains again showing the highest MICs (512 and 1,024 mg/liter, respectively). All of the variants expressed in *E. coli* DH10B except for the WT and the Y105F and -W variants showed a reduction in the MIC for piperacillin (≤32 mg/liter) when combined with 4 mg/liter of tazobactam. All were susceptible to penem-1 (39) in a fixed combination of 4-mg/liter inhibitor with piperacillin (MIC = 2 mg/liter). The Y105F and -W variant strains demonstrated higher MICs to ceftazidime (MIC 2 mg/liter) than the other variants (0.5 mg/liter). Some variants also had higher MICs against cephalothin (32 mg/liter, versus 64 mg/liter for WT): Y105F, -M, -N, -P, -Q, -R, -V, and -W. All strains remained susceptible to ceftriaxone.

SHV Y105 variant expression determined by Western blotting. We used a polyclonal antibody to assess steady-state production of β-lactamase by the Y105 variants to help interpret the MIC findings (18, 22–24, 36, 37). These antibodies have previously been characterized and are known to recognize several key epitopes in SHV. These include amino acids at the Ambler positions ABL 28 to 38, 42 to 54, 88 to 100, 102 to 114, 170 to 182, 186 to 194, 202 to 210, and 276 to 288 (20). In the epitope spanning amino acids 102 to 114, alanine and X-Scan analysis demonstrated that D104, Y105, P107, and S109 are essential residues for antibody recognition. The fact that the antibody is polyclonal in nature and recognizes multiple epitopes ensures that a single amino acid substitution will not influence recognition and allows one to use it to assess the overall expression of these SHV variant proteins. Notably, the SHV-1 polyclonal antibody does not recognize TEM-1, the class A β-lactamase of greatest homology to SHV (23), nor is there nonspecific binding to other cellular proteins (Fig. 2, *E. coli* DH10B negative control). All variants except for the T variant were expressed in amounts similar to that of the WT (Fig. 2). The T variant was expressed at a level of about 13% of that of the wild type. In addition, the F variant was expressed well, exceeding the amount expressed by the WT-producing strains by 16%. Protein expressed is processed protein in the periplasm (41).

Kinetics of SHV Y105 variants with substrates and inhibitors. Steady-state kinetic parameters were determined for the WT and the Y105E, -M, -R, and -F variants based on the observed MICs, the relative expression levels, and the nature of the side chain (size, charge, and hydrophobicity). Overall, the Y105E, -F, -M, and -R variants had reduced catalytic efficiency toward ampicillin (Table 4), with catalytic efficiencies of 5, 59, 34, and 12% activity, respectively, compared to that of the WT enzyme. The Y105E variant especially had a very large K_m toward this substrate but a preserved k_{cat}, accounting for the low catalytic efficiency. This trend was also observed with nitrocefin, with the Y105E variant showing a higher K_m toward this substrate. In this case, the Y105F variant actually had a lower K_m than the wild-type enzyme and a preserved catalytic efficiency. For cephalothin, the Y105F variant showed a dramatically lower K_m than the

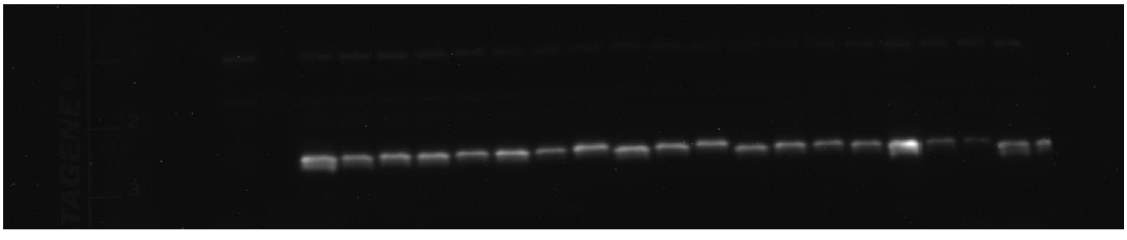

FIG 2 Western blots of Y105 variants for assessment of SHV β-lactamase expression levels.

TABLE 4 Kinetic constants for selected Y105 variants and substrates[a]

SHV	Nitrocefin			Ampicillin			Cephalothin		
	k_{cat} (s^{-1})	K_m (μM)	k_{cat}/K_m (s^{-1} μM^{-1})	k_{cat} (s^{-1})	K_m (μM)	k_{cat}/K_m (s^{-1} μM^{-1})	k_{cat} (s^{-1})	K_m (μM)	k_{cat}/K_m (s^{-1} μM^{-1})
WT	$(2.1 \pm 0.4) \times 10^2$	19 ± 2	11 ± 1	$(3.1 \pm 0.9) \times 10^3$	$(1.8 \pm 0.3) \times 10^1$	17 ± 2	$(5 \pm 1) \times 10^1$	26 ± 4	2.0 ± 0.2
Y105E	$(1.2 \pm 0.2) \times 10^2$	$(1.0 \pm 0.1) \times 10^2$	1.2 ± 0.1	$(1.4 \pm 0.7) \times 10^2$	$(1.5 \pm 0.6) \times 10^3$	0.9 ± 0.1	11 ± 3	7.2 ± 0.9	1.5 ± 0.2
Y105F	$(1.2 \pm 0.4) \times 10^2$	11 ± 2	11 ± 2	$(2.4 \pm 0.7) \times 10^3$	$(2.4 \pm 0.5) \times 10^2$	10 ± 1	20 ± 7	6 ± 2	3.3 ± 0.8
Y105 M	$(1.5 \pm 0.3) \times 10^2$	22 ± 3	6.6 ± 0.6	$(7 \pm 1) \times 10^2$	$(1.2 \pm 0.1) \times 10^2$	5.7 ± 0.4	12 ± 2	31 ± 4	0.37 ± 0.03
Y105R	$(1.4 \pm 0.3) \times 10^2$	31 ± 4	4.4 ± 0.4	$(1.2 \pm 0.3) \times 10^3$	$(6 \pm 1) \times 10^2$	2.0 ± 0.2	$(3 \pm 1) \times 10^1$	$(8 \pm 2) \times 10^1$	0.40 ± 0.04

[a] Determinations of kinetic parameters were performed in triplicate, and values are reported as means and standard deviations.

WT enzyme and a 33% higher catalytic efficiency. The Y105E variant also showed a lower K_m and preserved catalytic efficiency toward cephalothin compared to the WT. The Y105M and particularly the Y105R variants had significantly elevated K_ms for cephalothin. Hydrolysis of cefoperazone was not determined directly, but a K_d was determined in a competition reaction with NCF (Table 5). Here again, the Y105F variant had the lowest K_d value and the Y105E variant had a very elevated K_d.

Next we assessed the inhibition properties of the variants with clavulanic acid and with a bicyclic penem inhibitor, penem-1. We measured the K_i by the Dixon method and then obtained timed inactivation measurements of the inhibitors at [I] = K_i to determine a relative rate of inactivation, k_{inh}. The resulting K_i and k_{inh} values obtained are shown in Table 4 for the WT and the 4 variants studied for both clavulanic acid and penem-1. Both inhibitors behave in a competitive fashion. It is noted that the variants all have higher K_i values for both inhibitors, especially the Y105E variant. However, for clavulanic acid at least, the rate of inactivation is higher for the Y105E variant than for the WT enzyme. This is the trend for all of the variants in fact: the K_i is higher than that for the wild type, but the k_{inh} is higher.

For the penem inhibitor, the Y105E variant also demonstrates a significantly increased K_i (0.92 μM, versus 0.04 μM for WT). The k_{inh} could not be determined for the WT and the Y105R and -F variants by this manual method due to the rapid inactivation. However, the Y105E and -M variants showed lower, measurable rates of inactivation under these conditions, with k_{inh} values of 0.03 ± 0.02 and 0.15 ± 0.02 s^{-1}, respectively.

Raman spectroscopy. Spectra of the unreacted penem-1, the complex of SHV-1 and penem-1 in aqueous buffer, and a base hydrolysate of penem-1 are shown in Fig. 3. The intact penem exhibits a small, broad peak at 1,757 cm^{-1}, consistent with the carbonyl stretching frequency of the β-lactam ring. This is no longer present in the acyl enzyme or in the chemically hydrolyzed penem. The most prominent peak in the penem spectrum, at 1,687 cm^{-1}, is assigned to the methylidene double bond, and notably, the intensity of this band decreases in the acyl enzyme complex and in the hydrolyzed penem. Some unreacted compound is likely still present to account for the peaks in the latter spectrum. The most prominent feature in both the acyl enzyme spectrum and the hydrolysate appears as a broad band with maximal intensity at 1,622 cm^{-1} and is assigned to the enamine isomer of the 1,4-thiazepine ring (shown in reaction scheme Fig. 4, species 5). Previous studies with penem-2 and S130G SHV β-lactamase in aqueous solution and D_2O have demonstrated the presence of an exchangeable NH (ND) resonance at this frequency, consistent with the presence of a cyclic enamine (unpublished results). This study confirms the presence of a stable enamine inhibition intermediate when SHV β-lactamase is reacted with penem-1.

Molecular modeling of clavulanic acid Michaelis complex with Y105E and WT SHV. Due to its small size, clavulanic acid does not make many contacts with the active sites of class A β lactamases. The most important of these are the interaction of the carbonyl oxygen with the oxyanion hole formed by the backbone NH groups of Ser 70 and Ala 237 and the interaction of the C3′ carboxylate group with an H_2O molecule hydrogen bonded to Arg 244. Yet despite these limited interactions, multiple mutations exist that give rise to increased K_i values for this inhibitor. The molecular models of the Michaelis complex of clavulanic acid with SHV-1 (Fig. 5, thick gray lines) and with Y105E SHV (Fig. 5, thin gray lines) show that the inhibitor is in position for nucleophilic attack by Ser 70 with the β-lactam carbonyl in the oxyanion hole in the WT enzyme but that with the introduction of the Y105E mutation, the β-lactam ring is rotated away from its normal orientation and there is also rotation of the Arg 244 guanidinium toward the inhibitor, although not toward the newly positioned carboxylate. The oxyanion hole is distorted in the Y105E variant, with the Ser 70 backbone NH oriented away from its usual position.

Model of penem-2 in the SHV-1 active site. Previously, structures and models of tricyclic and bicyclic penem inhibitors have suggested that formation of the 7-membered thiazepine ring leads to an SHV-1 acyl enzyme complex in which there is a favorable interaction between the C6 aromatic side chain and the Y105 residue in SHV

TABLE 5 K_ds and inhibition constants for selected Y105 variants[a]

SHV	Cefoperazone K_d (μM)	Clavulanic acid		Penem-1	
		k_{inh} (s^{-1})	K_i (μM)	k_{inh} (s^{-1})	K_i (μM)
WT	40 ± 4	0.022 ± 0.005	1.1 ± 0.01	ND	0.040 ± 0.008
Y105E	$(2.8 \pm 0.3) \times 10^3$	0.11 ± 0.02	59 ± 3	0.03 ± 0.02	0.9 ± 0.3
Y105F	$(1.3 \pm 0.1) \times 10^2$	0.11 ± 0.03	2.4 ± 0.4	ND	0.073 ± 0.009
Y105 M	269 ± 3	0.13 ± 0.06	2.3 ± 0.5	0.15 ± 0.02	0.05 ± 0.02
Y105R	$(3.5 \pm 0.4) \times 10^2$	0.076 ± 0.009	7.2 ± 0.8	ND	0.130 ± 0.003

[a] Determinations of kinetic parameters were performed in triplicate, and values are reported as means and standard deviations. ND, not determined.

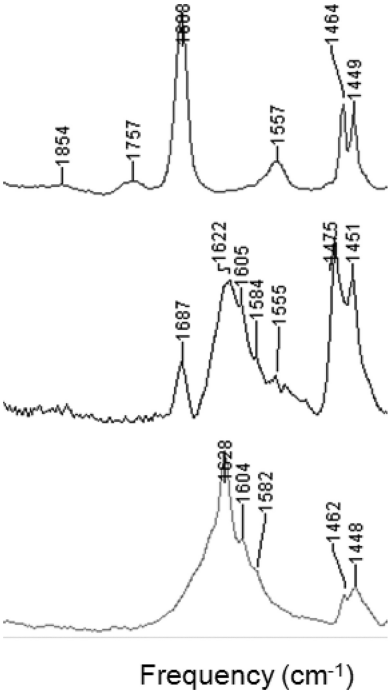

FIG 3 Raman spectra of penem-1, penem-1 acyl enzyme complex, and base hydrolysate. Top, Raman vibrational difference spectrum of penem-1 at 4 mM in water with water subtracted; middle, SHV-1–penem-1 acyl enzyme complex with SHV-1 protein subtracted; bottom, penem-1 at 4 mM in 1 N NaOH with NaOH subtracted.

(29, 32, 44). Models of the acyl enzyme complex of penem-2 with both WT SHV and the Y105 variants were prepared (Fig. 6).

The mutations at position 105 do not introduce large structural changes in the active sites of SHV-1 enzyme–penem-2 complexes (average root mean square deviation, 0.8 Å). In our model, we maintained the stereochemistry at C6 in the R configuration as in previous SHV structures and models with like inhibitors, and the oxygen of the acyl moiety carbonyl is pointing outside the oxyanion hole. However, unlike in the SHV-1–penem-4 structure ONG, our model indicates that the intermediate is rotated such that there is a 6.5-Å distance between the Y105 residue and the bicyclic side chain of penem-2. Thus, the favorable aromatic-aromatic interactions observed in X-ray structures between the Y105 aromatic ring and the bicyclic side chain of penem-2 are not seen here.

DISCUSSION

The role of residue 105 in class A enzymes has been debated in the β-lactamase literature for some time (6, 8, 15, 34, 37). It is in a loop region of the class A enzymes at the entrance of the active site and has important neighbors, such as an aspartate residue at position 104 that can undergo substitution by lysine, resulting in an extended-spectrum phenotype (1). Early mutagenesis work showed that in the class A β lactamase of *Bacillus licheniformis*, the F variant was as active as the WT, suggesting that the hydroxyl group was not necessary for substrate recognition (15). The fully active Y105C variant of the class A β lactamase of *B. cereus* suggested that hydrophobicity but not aromaticity was necessary at this position (6). Residue 105 is thought to be important in the alignment of substrates for hydrolysis and of clavulanic acid for its protonation prior to secondary ring opening. Natural examples to support this notion include the G105-containing class A β lactamase of *Staphylococcus albus* that is resistant to inhibition (34). Also, enzymes that lack an arginine in the vicinity of 244 are thought to require an aromatic residue at position 105 in order to be inhibited by clavulanate (34). The aromatic residue typically found at position 105 is thought to provide hydrophobic interactions that align the clavulanic acid clavam ring oxygen for protonation, although this has never been examined in non-KPC class A enzymes. More recent studies utilizing molecular dynamics simulations and nuclear magnetic resonance (NMR) have looked at the Y105 position in TEM β-lactamase and concluded that the residue has "higher than average flexibility" and that the conformation of the side chain is different in the apoenzyme and the enzyme interacting with substrates (9, 10). This contrasts with crystal structures of apo-SHV alone (26) and in complex with tazobactam (25), the penicillin sulfone inhibitor LN-1-255 (38), and two penem inhibitors where the conformation of Y105 remains the same (32). Only in the meropenem-bound SHV is residue Y105 rotated by approximately 90 degrees toward the entrance of the active site (33). Limited crystal structure data and molecular models of penem inhibitors have indicated that the Y105 in SHV provided van der Waals interactions that stabilized the acyl enzyme complex (29, 44).

Multiple substitutions are tolerated at position 105 but result in reduced catalytic efficiency. The Ambler 105 position in class A β lactamases is not a strictly conserved site, although many class A enzymes have a tyrosine or tryptophan at this position. Of note, the class A carbapenemase of *Klebsiella pneumoniae*, KPC, contains a tryptophan at the 105 site and is relatively resistant to inhibition by the traditional class A inhibitors clavulanic acid, sulbactam, and tazobactam. In both TEM and KPC, mutagenesis studies have shown that aromatic substitutions and Asn are best tolerated in terms of preserved enzymatic activity. In the case of KPC, all substitutions at position 105 result in enzymes that remain active toward imipenem hydrolysis, but Y105F and -N show increased activity compared to the WT (37). Molecular dynamics simulations of TEM β-lactamase suggest that long branch chain residues exhibit greater flexibility that deters substrate binding (9). In the case of SHV, most substitutions result in functional penicillinases, with the exception of the Y105A and -L substitutions. The Y105F and -W substitutions yield variants that have high MICs toward ampicillin, with the Y105F substitution being the most active. As in TEM, this indicates that the OH is not needed for activity. When further compared to TEM, which has 68% amino acid identity, fewer SHV variants retain high-level activity versus ampicillin and cefazolin. Overall, the SHV variants exhibited higher affinity for cephalothin but had decreased hydrolysis rates when contrasted with comparable TEM enzymes.

These findings underscore the significance of the 105 site in positioning both substrates and inhibitors in a variety of important class A β-lactamases, now including SHV. Interactions with an aromatic 105 residue should be considered in the design of future β-lactams and β-lactamase inhibitors for class A enzymes.

Substitutions at position 105 may result in perturbations of the oxyanion hole and side chain Arg 244, leading to reduced affinity for substrates and inhibitors. In our selection of variants to study, we chose the Y105E variant as a representative enzyme that had lost function, and, not surprisingly, it also exhibited the highest K_m and K_i values among the enzymes studied kinetically. The 10-fold increase in K_m for ampicillin is responsible for de-

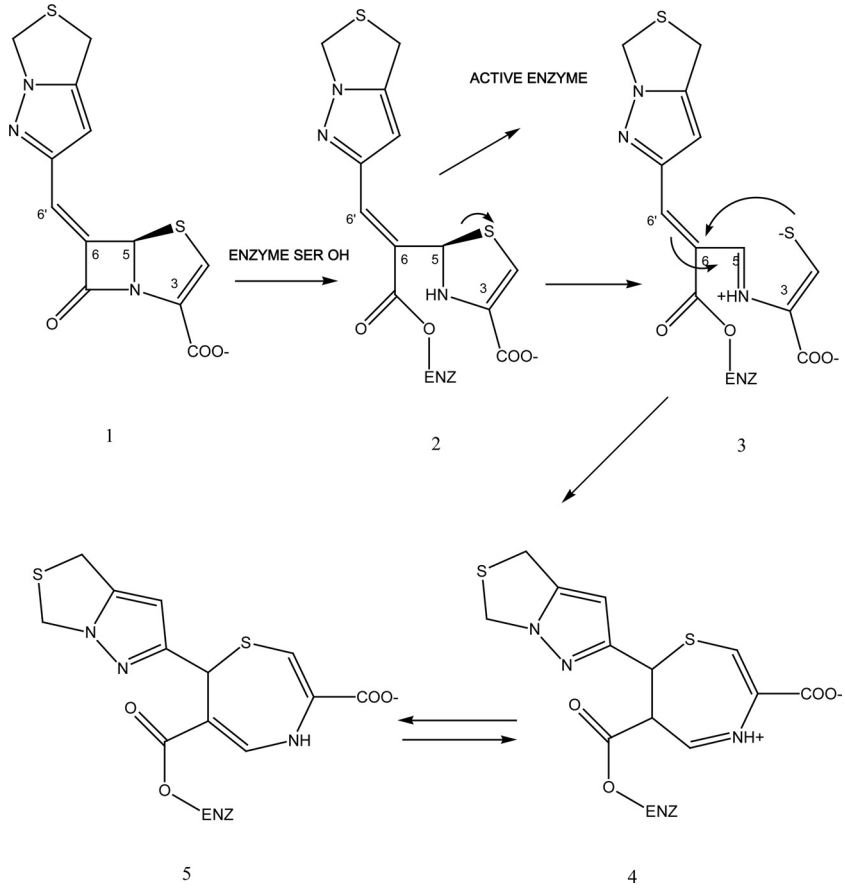

FIG 4 Reaction scheme for inhibition of serine β-lactamases with penem-1 inhibitor, showing the formation of the 1,4-thiazepine intermediates detectable by Raman vibrational spectroscopy (species 5).

creased catalytic efficiency of Y105E SHV. Molecular modeling studies of the Henri-Michaelis-Menton complexes of clavulanic acid with SHV-1 and Y105E SHV suggest that some substitutions at position 105 result in changes in binding in the two key contact points in the class A active site for small-molecule β-lactam inhibitors: the oxyanion hole (backbone NH of Ser 70 and Ala 237) and Arg 244. Such alterations in the movement or flexibility of active-site residues far from position 105 have also been observed in TEM variants with changes at the 105 site (10) and postulated in KPC-2 (35, 37). It was hypothesized previously that the residue at position 105 was important for positioning of clavulanic acid for protonation prior to secondary ring opening in the formation of the linear inhibitor intermediate (34). In addition, other inhibitor resistance mutations noted in class A β-lactamases have also been associated with alterations in the oxyanion hole and the position of Arg 244: M69I, -L, and -V; S130G; and D276 (reviewed in reference 12). When combined with the experimental data, this suggests that the glutamate substitution leads to a change in the initial binding affinity for both substrates and inhibitors. However, the rate of inactivation is relatively less affected than the K_i, suggesting that repositioning of Arg 244 has not affected the protonation of the clavam ring oxygen enough to cause an effect on the inactivation rate. Such long-range interactions have important implications in the design of inhibitors of these flexible and adaptable enzymes (11, 12).

Susceptibility to bicyclic penem inhibitors is preserved in the Y105 variants of SHV. Previous crystal structures of related bicyclic penem inhibitors in SHV have shown stabilizing van der Waals interactions with Y105, suggesting that resistance to such inhibitors could occur with mutations at position 105. Raman studies of the WT enzyme confirm the presence of a stable enamine inhibition intermediate with penem-1 and -2 but cannot reveal interactions with residue Y105. Our data show, however, that all of the *E. coli* DH10B strains expressing Y105 SHV variants are fully susceptible to the penem inhibitor in a fixed combination with piperacillin, tested according to previously published methods for a similar inhibitor (39). Our models, which are based on the crystal structures for these related compounds (1ONG), show that the inhibitor complex becomes positioned such that the bicyclic side chain faces away from residue 105. Each residue examined occupies the same position as the WT tyrosine, and there are no additional structural perturbations noted in the variants compared to the WT. Hence, mutations at position Y105 do not appear to affect the stabilizing interactions present in the SHV–penem-1 complexes.

Aromatic substitutions preserve activity, whereas glutamate reduces binding affinity of substrates and inhibitors. Four variants were selected for additional detailed kinetic analysis based on the observed MICs, relative expression levels, and the nature of the side chain (size, charge, and hydrophobicity). Similar to results of other studies that have examined position 105 in class A β-lactamases such as the closely related TEM enzyme and the carbapen-

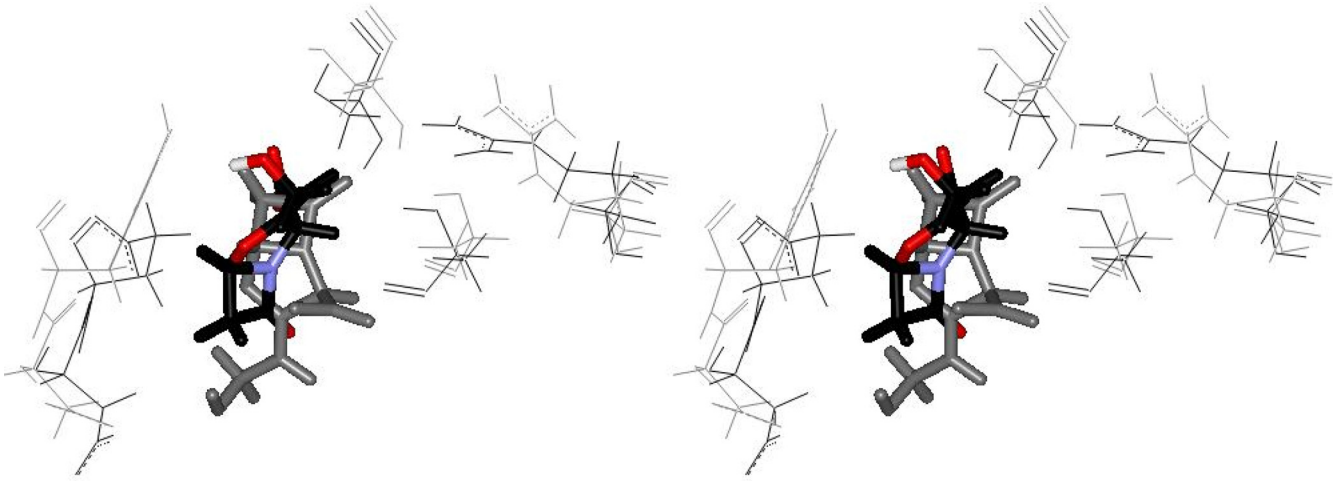

FIG 5 Stereo image of models of clavulanic acid Michaelis complexes with the Y105E variant (black structure) and the WT (gray structure). The superimposed models demonstrate that in WT SHV-1, clavulanic acid is oriented with its β-lactam carbonyl in the oxyanion hole formed by the backbone NH groups of S 70 and A 237. The Y105 residue forms a hydrophobic wall within the active site. In the Y105E variant, the modeled Michaelis complex of clavulanic acid suggests that the inhibitor is flipped so that the carbonyl oxygen is not located in the oxyanion hole. The oxyanion hole is altered, with the S 70 NH pointing away from its usual position. The glutamate side chain may cause steric hindrance in the active site. Also, the R244 side chain is positioned differently in the Y105E variant. These perturbations could account for the increased K_i toward clavulanic acid observed with this variant.

emase, KPC-2, most of the variants with changes at position 105 retain activity but the aromatic-substituted (Y105F and -W) enzymes are most active toward substrates. Kinetic analyses demonstrate that the variants possess a range of apparent substrate and inhibitor affinities compared to the WT SHV enzyme, as well as a range of hydrolysis and relative inhibition rates. *E. coli* strains expressing the E variant are very susceptible to ampicillin, and they are also resistant to clavulanic acid, consistent with our measured K_m and K_i values. However, the k_{inh} value is greater than for the WT enzyme, suggesting that the ampicillin susceptibility and inhibitor resistance both result from decreased enzyme affinity for these β-lactam molecules. This has been observed previously with other inhibitor-resistant SHVs such as S130G and R244S SHV (17, 43). Our Henri-Michaelis-Menten molecular models of the WT and the Y105 mutant show an alteration in the geometry of the oxyanion hole that leads to poor docking of the carbonyl. This contrasts with recent studies of KPC in which the Y105E variant has low activity and no resistance to clavulanic acid; however, the Y105D variant shows high MIC values for clavulanic acid and sulbactam (37). Differences in overall active-site size and geometry may account for this.

Concluding remarks. Position 105 in the class A β-lactamases continues to be an interesting and important site in substrate and inhibitor recognition. The role of this residue in SHV is similar to what is seen in related enzymes such as TEM and KPC, in that it likely has far-reaching interactions that affect key β-lactam recognition sites in these enzymes, such as the oxyanion hole. It may also affect catalysis and inhibition by altering the pK_a of the clavulanic acid clavam ring oxygen, which is likely to be protonated prior to secondary ring opening (42). However, the substrate and inhibitor specificities are different depending on the particular

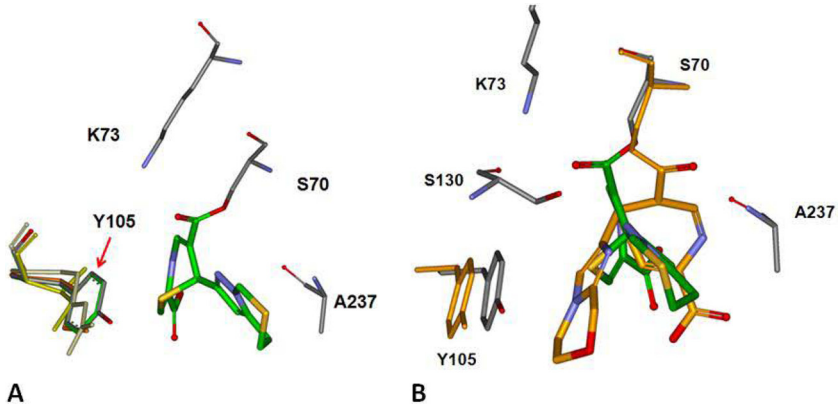

FIG 6 (A) Seven-membered ring intermediate of penem-2 modeled in the active site of SHV-1. Unlike in the PDB structure ONG (protein in gray and intermediate with orange-colored carbons), the SHV-1 intermediate with penem-2 is rotated such that there is no interaction between residue 105 and the bicyclic side chain. Thus, the favorable aromatic-aromatic interactions observed in X-ray structures between the Y105 aromatic ring and the bicyclic side chain of the penem are not seen here. The bicyclic substituent is pushed back more than 3 Å (more than 6.5 Å between the Y105 and the inhibitor). (B) Seven-membered ring intermediate of penem-2 (carbon atoms colored green) modeled in the active sites of SHV-1 (green) and the SHV Y105K (gray) and SHV Y105E (gray) variants. The E and K side chains assume the same position in the active site as the native Y.

substitution in a given class A enzyme. Aromatic substitutions such as F and W do appear to maintain the penicillinase phenotype of SHV as well as susceptibility to clavulanic acid.

ACKNOWLEDGMENTS

This work was funded by the Department of Veterans Affairs Merit Review program (M.J.S.).

We thank Robert Bonomo for critical reading of the manuscript.

REFERENCES

1. **Bethel CR, et al.** 2006. Role of Asp104 in the SHV β-lactamase. Antimicrob. Agents Chemother. **50**:4124–4131.
2. **Bradford MM.** 1976. A rapid and sensitive method for the quantitation of microgram quantities of protein utilizing the principle of protein-dye binding. Anal. Biochem. **72**:248–254.
3. **Bush K.** 2010. Alarming β-lactamase-mediated resistance in multidrug-resistant Enterobacteriaceae. Curr. Opin. Microbiol. **13**:558–564.
4. **Bush K, Jacoby GA.** 2010. Updated functional classification of β-lactamases. Antimicrob. Agents Chemother. **54**:969–976.
5. **CLSI.** 2011. Performance standards for antimicrobial susceptibility testing; twenty-first informational supplement. M100-S21. CLSI, Wayne, PA.
6. **Di Gleria K, Halliwell CM, Jacob C, Hill HA.** 1997. Site-specific introduction of an electroactive label into a non-electroactive enzyme (β-lactamase I). FEBS Lett. **400**:155–157.
7. **Dixon M.** 1965. Graphical determination of equilibrium constants. Biochem. J. **94**:760–762.
8. **Doucet N, De Wals PY, Pelletier JN.** 2004. Site-saturation mutagenesis of Tyr-105 reveals its importance in substrate stabilization and discrimination in TEM-1 β-lactamase. J. Biol. Chem. **279**:46295–46303.
9. **Doucet N, Pelletier JN.** 2007. Simulated annealing exploration of an active-site tyrosine in TEM-1 β-lactamase suggests the existence of alternate conformations. Proteins **69**:340–348.
10. **Doucet N, Savard PY, Pelletier JN, Gagné SM.** 2007. NMR investigation of Tyr105 mutants in TEM-1 β-lactamase: dynamics are correlated with function. J. Biol. Chem. **282**:21448–21459.
11. **Drawz SM, et al.** 2009. The role of a second-shell residue in modifying substrate and inhibitor interactions in the SHV β-lactamase: a study of ambler position Asn276. Biochemistry **48**:4557–4566.
12. **Drawz SM, Bonomo RA.** 2010. Three decades of β-lactamase inhibitors. Clin. Microbiol. Rev. **23**:160–201.
13. **Dubois V, et al.** 2004. SHV-49, a novel inhibitor-resistant β-lactamase in a clinical isolate of Klebsiella pneumoniae. Antimicrob. Agents Chemother. **48**:4466–4469.
14. **Dubois V, et al.** 2008. Molecular and biochemical characterization of SHV-56, a novel inhibitor-resistant β-lactamase from Klebsiella pneumoniae. Antimicrob. Agents Chemother. **52**:3792–3794.
15. **Escobar WA, Miller J, Fink AL.** 1994. Effects of site-specific mutagenesis of tyrosine 105 in a class A β-lactamase. Biochem. J. **303**:555–558.
16. **Frase H, Toth M, Champion MM, Antunes NT, Vakulenko SB.** 2011. Importance of position 170 in the inhibition of GES-type β-lactamases by clavulanic acid. Antimicrob. Agents Chemother. **55**:1556–1562.
17. **Helfand MS, et al.** 2003. Understanding resistance to β-lactams and β-lactamase inhibitors in the SHV β-lactamase: lessons from the mutagenesis of SER-130. J. Biol. Chem. **278**:52724–52729.
18. **Helfand MS, Hujer AM, Sönnichsen FD, Bonomo RA.** 2002. Unexpected advanced generation cephalosporinase activity of the M69F variant of SHV β-lactamase. J. Biol. Chem. **277**:47719–47723.
19. **Helfand MS, et al.** 2003. Following the reactions of mechanism-based inhibitors with β-lactamase by Raman crystallography. Biochemistry **42**: 13386–13392. (Erratum, **42**:15398).
20. **Hujer AM, Bethel CR, Bonomo RA.** 2004. Antibody mapping of the linear epitopes of CMY-2 and SHV-1 β-lactamases. Antimicrob. Agents Chemother. **48**:3980–3988.
21. **Hujer AM, Hujer KM, Bonomo RA.** 2001. Mutagenesis of amino acid residues in the SHV-1 β-lactamase: the premier role of Gly238Ser in penicillin and cephalosporin resistance. Biochim. Biophys. Acta **1547**:37–50.
22. **Hujer AM, Hujer KM, Helfand MS, Anderson VE, Bonomo RA.** 2002. Amino acid substitutions at Ambler position Gly238 in the SHV-1 β-lactamase: exploring sequence requirements for resistance to penicillins and cephalosporins. Antimicrob. Agents Chemother. **46**:3971–3977.
23. **Hujer AM, Page MG, Helfand MS, Yeiser B, Bonomo RA.** 2002. Development of a sensitive and specific enzyme-linked immunosorbent assay for detecting and quantifying CMY-2 and SHV β-lactamases. J. Clin. Microbiol. **40**:1947–1957.
24. **Kitchel B, et al.** 2010. Genetic factors associated with elevated carbapenem resistance in KPC-producing *Klebsiella pneumoniae.* Antimicrob. Agents Chemother. **54**:4201–4207.
25. **Kuzin AP, et al.** 2001. Inhibition of the SHV-1 β-lactamase by sulfones: crystallographic observation of two reaction intermediates with tazobactam. Biochemistry **40**:1861–1866.
26. **Kuzin AP, et al.** 1999. Structure of the SHV-1 β-lactamase. Biochemistry **38**:5720–5727.
27. **Lavilla S, et al.** 2008. Prevalence of qnr genes among extended-spectrum β-lactamase-producing enterobacterial isolates in Barcelona, Spain. J. Antimicrob. Chemother. **61**:291–295.
28. **Manageiro V, Ferreira E, Albuquerque L, Bonnet R, Caniça M.** 2010. Biochemical study of a new inhibitor-resistant β-lactamase, SHV-84, produced by a clinical Escherichia coli strain. Antimicrob. Agents Chemother. **54**:2271–2272.
29. **Mansour TS, et al.** 2007. On the absolute configuration in 1,4-dihydrothiazepine covalent complexes derived from inhibition of class A and C β-lactamases with 6-methylidene penems. ChemMedChem **2**:1713–1716.
30. **Mendonça N, et al.** 2008. The Lys234Arg substitution in the enzyme SHV-72 is a determinant for resistance to clavulanic acid inhibition. Antimicrob. Agents Chemother. **52**:1806–1811.
31. **Mendonça N, Nicolas-Chanoine MH, Caniça M.** 2009. Diversity of the bla(SHV) genes. Diagn. Microbiol. Infect. Dis. **65**:439–446.
32. **Nukaga M, et al.** 2003. Inhibition of class A and class C β-lactamases by penems: crystallographic structures of a novel 1,4-thiazepine intermediate. Biochemistry **42**:13152–13159.
33. **Nukaga M, et al.** 2008. Inhibition of class A β-lactamases by carbapenems: crystallographic observation of two conformations of meropenem in SHV-1. J. Am. Chem. Soc. **130**:12656–12662.
34. **Page MG.** 2000. β-Lactamase inhibitors. Drug Resist. Updat. **3**:109–125.
35. **Papp-Wallace KM, Distler AM, Kasuboski C, Taracila M, Bonomo RA.** 2010. Inhibitor resistance in the KPC-2 β-lactamase, a preeminent property of this class A β-lactamase. Antimicrob. Agents Chemother. **54**:890–897.
36. **Papp-Wallace KM, et al.** 2010. Substrate selectivity and a novel role in inhibitor discrimination by residue 237 in the KPC-2 β-lactamase. Antimicrob. Agents Chemother. **54**:2867–2877.
37. **Papp-Wallace KM, et al.** 2010. Elucidating the role of Trp105 in the KPC-2 β-lactamase. Protein Sci. **19**:1714–1727.
38. **Pattanaik P, et al.** 2009. Strategic design of an effective β-lactamase inhibitor: LN-1-255, a 6-alkylidene-2′-substituted penicillin sulfone. J. Biol. Chem. **284**:945–953.
39. **Petersen PJ, et al.** 2009. Establishment of in vitro susceptibility testing methodologies and comparative activities of piperacillin in combination with the penem β-lactamase inhibitor BLI-489. Antimicrob. Agents Chemother. **53**:370–384.
40. **Prinarakis EE, Miriagou V, Tzelepi E, Gazouli M, Tzouvelekis LS.** 1997. Emergence of an inhibitor-resistant β-lactamase (SHV-10) derived from an SHV-5 variant. Antimicrob. Agents Chemother. **41**:838–840.
41. **Rholl DA, et al.** 2011. Molecular Investigations of PenA-mediated β-lactam resistance in Burkholderia pseudomallei. Front. Microbiol. **2**:139.
42. **Swarén P, et al.** 1999. X-ray structure of the Asn276Asp variant of the Escherichia coli TEM-1 β-lactamase: direct observation of electrostatic modulation in resistance to inactivation by clavulanic acid. Biochemistry **38**:9570–9576.
43. **Thomson JM, Distler AM, Prati F, Bonomo RA.** 2006. Probing active site chemistry in SHV β-lactamase variants at Ambler position 244. Understanding unique properties of inhibitor resistance. J. Biol. Chem. **281**: 26734–26744.
44. **Venkatesan AM, et al.** 2006. Structure-activity relationship of 6-methylidene penems bearing 6,5 bicyclic heterocycles as broad-spectrum β-lactamase inhibitors: evidence for 1,4-thiazepine intermediates with C7 R stereochemistry by computational methods. J. Med. Chem. **49**:4623–4637.
45. **Yigit H, et al.** 2001. Novel carbapenem-hydrolyzing β-lactamase, KPC-1, from a carbapenem-resistant strain of Klebsiella pneumoniae. Antimicrob. Agents Chemother. **45**:1151–1161. (Erratum, **52**:809, 2008).
46. **Yigit H, et al.** 2003. Carbapenem-resistant strain of Klebsiella oxytoca harboring carbapenem-hydrolyzing β-lactamase KPC-2. Antimicrob. Agents Chemother. **47**:3881–3889.